Journal of Mathematical Modeling
Vol. 6, No. 1, 2018, pp. 105-122

JMM

Biorthogonal wavelet-based full-approximation schemes for the numerical solution of elasto-hydrodynamic lubrication problems

Siddu C. Shiralashetti[†], **Mounesha H. Kantli**[‡*] **and Aravind B. Deshi**[†]

[†]*Department of Mathematics, Karnatak University Dharwad-580003, India*

[‡]*Department of Mathematics, KLE Society's J. T. College, Gadag-582101, India*

[†]*Department of Mathematics, KLECET Chikodi-591201, India*

emails: shiralashettisc@gmail.com, mkantli@gmail.com, aravind42d@gmail.com

Abstract. Biorthogonal wavelet-based full-approximation schemes are introduced in this paper for the numerical solution of elasto-hydrodynamic lubrication line and point contact problems. The proposed methods give higher accuracy in terms of better convergence with low computational time, which have been demonstrated through the illustrative problems.

Keywords: CDF wavelets filter coefficients, Full-approximation scheme, Elasto-hydrodynamic lubrication problems.
AMS Subject Classification: 34K28, 76D07, 97N40.

1 Introduction

In numerical approximations, wavelets are used as efficient tools for the rapid numerical applications in differential equations. They are widely and efficiently applied in engineering field for example signal analysis, image processing, etc. Subsequently, the development of multiresolution analysis and the fast wavelet transforms by Avudainayagam and Vani [2] and

*Corresponding author.

Received: 21 June 2016 / Revised: 21 September 2016 / Accepted: 10 October 2016.
DOI 10.22124/jmm.2018.5019.1059

Bujurke et al. [6–8] led to extensive research in wavelet multigrid schemes to solve certain differential equations arising in fluid dynamics. Beylkin et al. [3] observed that wavelet decomposition can be used to approximate the system of highly sparse matrices. The biorthogonal wavelets exhibit both higher compression factors and faster execution than corresponding orthogonal wavelets at comparable accuracy. Thus, they presented a highly competitive, alternative to Daubechies wavelets and Coiflets for applications in numerical approximations. For finest results, the wavelets should have several vanishing moments, good advantages and a support as small as possible. Faster algorithms are potential if the scaling function also has several vanishing moments (except for the zeroth moment, which must be 1). Orthogonal wavelets are expected to give the best compression ratio, while biorthogonal wavelets lead to faster decomposition algorithms at slightly reduced compression.

Non-linearity is essential in the mainstream of physical phenomena and engineering science processes, resulting in non-linear differential equations. In fact, these non-linear equations are usually difficult to solve, since no common procedure works worldwide. Hence each separate equation has to be studied as a distinct problem. In the particular interest, the non-linear elliptic type equations are notably fluid flow problems such as, elasto-hydrodynamic lubrication (EHL) problems. Solutions to this type of problems are usually required more CPU time with slow convergence.

The EHL is one of the important topics in tribology. It is a form of fluid film lubrication where the elastic deformation of the contacting surface, under heavy load, plays the dominant role. The most common types of such bearings are contacting surfaces with low geometric conformity where load is concentrated in a small region. These are rolling bearings, gears, cams, synovial joints and others. The deformation of the bearing surface results in changing the geometry of the lubricanting film which is coupled with the changes in pressure developed. Salient features of EHL are presented by Dowson and Higginson [11]. The Mathematical model consists of Reynolds equation for the pressure distribution, integral equation for surface deformation, force balance equation with applied load, pressure dependent density and viscosity of the lubricants. These equations are considered together with appropriate boundary conditions. Usually, many researchers use the finite difference, finite element, Newton and other methods for the solution of line as well as point contact EHL problems. The innovative work of Leeds group (Dowson, Higginson and their associates) and also that of Netherland (Lubrecht, Venner and their associates), the work of many dedicated researchers on EHL has exciting history. The appearance of sharp pressure peak, the maximum pressure (the Petruservish spike [15]), near the outlet and corresponding dip in film thickness is of special interest in EHL due to its profound impact on lubrication of bearings. The review by Lugt and Moraes-Espejel [14] presents current activities, listing various methods used in the analysis, and predicts the useful future developments in EHL. Once we apply the finite difference/finite element method, the EHL governing equations are reduced to a system of nonlinear equations and it is difficult to get good accuracy with low computational time. In fact, the classical iterative methods (namely, Newton's method, Jacobi iterative method, Gauss-Seidel method, etc) are used to solve the problems with low accuracy in more computational time. The full-approximation scheme (FAS) is largely applicable in increasing the efficiency of the iterative methods to solve nonlinear system of algebraic equations. FAS is a well-founded numerical scheme for solving nonlinear system of equations for approximating given differential equation. In the history of numerical analysis, the development of effective iterative solvers for nonlinear systems of algebraic equations has been a significant research topic in computational engineering sciences. Nowadays it is recognized that FAS iterative solver is highly efficient for nonlinear differential equations introduced by Brandt [4]. For a detailed treatment of FAS see Briggs et al. [5]. An introduction of FAS is found in Hackbusch and Trottenberg [12], Wesseling [22] and Trottenberg et al. [19]. Many authors namely, Brandt [4] and Briggs et al. [5], applied the FAS to some class of differential equations. Lubrecht [13], Venner and Lubrecht [20], Zargari [23] and others have the significant contributions in EHL problems. The ill-conditioned matrices are arising in the solution of system of algebraic equations. The suitable remedy is multigrid scheme for such matrices namely; standard multigrid, orthogonal wavelet multigrid and biorthogonal multigrid. But there are large classes of matrices occurring in the modelling of problems of interest, which are not amenable even to these latest non stationary iterative schemes with classical multigrids (standard multigrid and orthogonal wavelet multigrid) for their solutions. But biorthogonal wavelet-based multigrid schemes are found to be effective. Zargari et al. [23] used decoupled scheme, one of the methods not yielding converging solution for some set of physical parameters. Biorthogonal wavelet-based multigrid schemes provide some remedy in such challenging cases. Sweldens [18] highlights effectively the construction of biorthogonal wavelet filters for the solution of large class of ill-conditioned system.

In this paper, the governing equations of EHL line and point contact problems are analyzed by discretizing the equations using finite difference scheme. The resulting nonlinear system of algebraic equations is solved using Newton's method, one of the efficient numerical methods. As the Jacobian is full in EHL problems, the convergence of the iteration is not guaranteed and takes large number of iterations to converge. It is essential to find effective multigrid schemes. In EHL, matrices are dense with non-smooth diagonal and smooth away from the diagonal. This smoothness of the matrix transforms into smallness in wavelet transform and facilitates in the design or construction of efficient multigrid scheme using biorthogonal discrete wavelet transform (BDWT). This matrix designed and implemented by Ruch and Fleet [17] for decomposition and reconstruction of the given signals and images. Using these decomposition and reconstruction matrices we introduced restriction and prolongation operators, respectively, in the implementation of biorthogonal wavelet full-approximation schemes (BWFAS).

This paper is divided as follows; Biorthogonal wavelets are given in Section 2. Section 3 deals with the method of solution using intergrid operators. Numerical findings of the test problems are presented in Section 4. Finally, conclusions of the proposed work are discussed in Section 5.

2 Biorthogonal wavelets

Biorthogonality is a concept for which, engineers are not much aware. In signal processing, especially in wavelets, however, it is a notion which nobody can ignore. Biorthogonal wavelets are the working horse overdue many profitable claims like finger print image compression. In various filtering applications we need filters with symmetrical coefficients to accomplish linear phase. None of the orthogonal wavelet systems apart from Haar are having symmetrical coefficients. But Haar is too insufficient for countless practical applications. Biorthogonal wavelet system can be premeditated to have this property. That is our motivation for manipulative such wavelet system. To understand the entire theory more let us primarily consider some biorthogonal filters and construct corresponding scaling functions and wavelet functions. Spline-based biorthogonal wavelet systems are more easy to construct [10].

2.1 Biorthogonal wavelets: Cohen-Daubechies-Feauveau wavelets (CDF)

In [17], Ruch and Fleet build a biorthogonal structure called dual multiresolution analysis that allows for the construction of symmetric scaling filters and that can incorporate spline functions. They used instead of scaling (h) and wavelet (g) filters, the new construction which yields scaling ($\tilde{h}$)

and wavelet ($\tilde{g}$) filters as decomposition and reconstruction. Instead of a single scaling function $\phi(x)$ and wavelet function φ(x), the dual multiresolution analysis requires a pair of scaling functions ϕ(x) and $\tilde{\phi}(x)$ related by a duality condition similarly, a pair of wavelet functions φ(x) and $\tilde{\varphi(x)}$. To construct the BDWT matrix, the same thing is used in to build the orthogonal discrete wavelet transform matrix. Due to excellent properties of biorthogonality and minimum compact support, CDF wavelets can be useful and convenient, providing guaranty of convergence and accuracy of the approximation in a wide variety of situations.

In this paper, we use CDF(2, 2) filter coefficients which are; Low pass filter coefficients: $h_{-1} = -\frac{\sqrt{2}}{8}$, $h_0 = \frac{\sqrt{2}}{4}$, $h_1 = \frac{3\sqrt{2}}{4}$, $h_2 = \frac{\sqrt{2}}{4}$, $h_3 = -\frac{\sqrt{2}}{8}$; High pass filter coefficients: $g_{-1} = \frac{\sqrt{2}}{4}$, $g_0 = -\frac{\sqrt{2}}{2}$, $g_1 = \frac{\sqrt{2}}{4}$ for decomposition matrix. Low pass filter coefficients: $\tilde{h}_{-1} = g_1$, $\tilde{h}_0 = -g_0$, $\tilde{h}_1 = g_{-1}$ High pass filter coefficients: $\tilde{g}_{-1} = -h_3$, $\tilde{g}_0 = h_2$, $\tilde{g}_1 = -h_1$, $\tilde{g}_2 = h_0$, $\tilde{g}_3 = -h_{-1}$ for reconstruction matrix.

2.2 Biorthogonal discrete wavelet transform (BDWT) matrix

The matrix formulation of the biorthogonal discrete wavelet transforms (BDWT), which play an important role in the biorthogonal wavelet method for the numerical computations. As we already know about the BDWT matrix and its applications in the wavelet method and is given in [18] as, decomposition matrix:

$$Dw = \begin{bmatrix} h_0 & h_1 & h_2 & h_3 & 0 & 0 & . & . & . & 0 & h_{-1} \\ g_0 & g_1 & 0 & 0 & . & . & . & . & . & 0 & g_{-1} \\ 0 & h_{-1} & h_0 & h_1 & h_2 & h_3 & 0 & . & . & . & 0 \\ 0 & g_{-1} & g_0 & g_1 & 0 & 0 & . & . & . & . & 0 \\ . & & & . & & & . & & & . & \\ . & & & . & & & . & & & . & \\ . & & & . & & & . & & & . & \\ h_2 & h_3 & 0 & 0 & . & . & . & 0 & h_{-1} & h_0 & h_1 \\ 0 & 0 & . & . & . & . & . & 0 & g_{-1} & g_0 & g_1 \end{bmatrix}_{N\times N},$$

and reconstruction matrix:

$$Rw = \begin{bmatrix} \tilde{h}_0 & \tilde{h}_1 & 0 & 0 & 0 & 0 & . & . & . & 0 & \tilde{h}_{-1} \\ \tilde{g}_0 & \tilde{g}_1 & \tilde{g}_2 & \tilde{g}_3 & . & . & . & . & . & 0 & \tilde{g}_{-1} \\ 0 & \tilde{h}_{-1} & \tilde{h}_0 & \tilde{h}_1 & 0 & 0 & 0 & . & . & . & 0 \\ 0 & \tilde{g}_{-1} & \tilde{g}_0 & \tilde{g}_1 & \tilde{g}_2 & \tilde{g}_3 & 0 & . & . & . & 0 \\ . & & & . & & & . & & & . & \\ . & & & . & & & . & & & . & \\ . & & & . & & & . & & & . & \\ 0 & 0 & 0 & 0 & . & . & . & 0 & \tilde{h}_{-1} & \tilde{h}_0 & \tilde{h}_1 \\ \tilde{g}_2 & \tilde{g}_3 & . & . & . & . & . & 0 & \tilde{g}_{-1} & \tilde{g}_0 & \tilde{g}_1 \end{bmatrix}_{N\times N}.$$

Using these matrices we introduce restriction and prolongation operators, respectively, based on multigrid restriction and prolongation operators detailed procedure explained in Section 3.

2.3 New biorthogonal discrete wavelet transform (NBDWT) matrix

Here, we developed NBDWT matrix similar to BDWT matrix in which by adding rows and columns consecutively with diagonal element as 1, which is built as, New decomposition matrix:

$$
NDw = \begin{bmatrix}
h_0 & 0 & h_1 & 0 & h_2 & 0 & h_3 & 0 & . & . & . & 0 & h_{-1} & 0 \\
0 & 1 & 0 & 0 & . & . & . & & & . & . & . & 0 \\
g_0 & 0 & g_1 & 0 & 0 & . & . & . & & 0 & 0 & 0 & g_{-1} & 0 \\
0 & 0 & 0 & 1 & 0 & . & . & . & & . & . & . & 0 \\
. & & & & . & & & & . & & & . & & \\
. & & & & . & & & & . & & & . & & \\
. & & & & . & & & & . & & & . & & \\
h_2 & 0 & h_3 & 0 & . & . & . & 0 & h_{-1} & 0 & h_0 & 0 & h_1 & 0 \\
0 & 0 & . & . & . & & & . & . & . & 0 & 1 & 0 & 0 \\
0 & 0 & . & . & . & . & . & 0 & g_{-1} & 0 & g_0 & 0 & g_1 & 0 \\
0 & 0 & . & . & . & & & . & . & . & & & 0 & 1
\end{bmatrix}_{N\times N},
$$

and New reconstruction matrix:

$$
NRw = \begin{bmatrix}
\tilde{h}_0 & 0 & \tilde{h}_1 & 0 & 0 & 0 & 0 & 0 & . & . & . & 0 & \tilde{h}_{-1} & 0 \\
0 & 1 & 0 & 0 & . & . & . & & & . & . & . & 0 \\
\tilde{g}_0 & 0 & \tilde{g}_1 & 0 & \tilde{g}_2 & 0 & \tilde{g}_3 & 0 & . & . & . & 0 & \tilde{g}_{-1} & 0 \\
0 & 0 & 0 & 1 & 0 & . & . & . & & . & . & . & 0 \\
. & & & & . & & & & . & & & . & & \\
. & & & & . & & & & . & & & . & & \\
. & & & & . & & & & . & & & . & & \\
0 & 0 & . & . & . & 0 & 0 & 0 & \tilde{h}_{-1} & 0 & \tilde{h}_0 & 0 & \tilde{h}_1 & 0 \\
0 & 0 & . & . & . & & & . & . & . & 0 & 1 & 0 & 0 \\
\tilde{g}_2 & 0 & \tilde{g}_3 & 0 & . & . & . & 0 & \tilde{g}_{-1} & 0 & \tilde{g}_0 & 0 & \tilde{g}_1 & 0 \\
0 & 0 & . & . & . & & & . & . & . & & & 0 & 1
\end{bmatrix}_{N\times N}.
$$

Using these matrices we introduced a new restriction and prolongation operators, respectively, based on multigrid restriction and prolongation operators detailed procedure explained in Section 3.

3 Method of solution

Consider the nonlinear partial differential equation. After discretizing the partial differential equation through the finite difference method, we get the system of nonlinear equations of the form,

$$
A(P_{ij}) = f_{ij}, \tag{1}
$$

where $i, j = 1, 2, \ldots, N$, which have $N \times N$ equations with $N \times N$ unknowns. Solve Eq. (1) through Gauss Seidel (GS) iterative method, we get approximate solution $\tilde{P}_{ij}$. Approximate solution containing some error, therefore required solution equals to sum of approximate solution and error. There are many methods to minimize such error to get the accurate solution. Some of them are FAS, BWFAS, NBWFAS, etc. Now we are discussing the method of solution of the above mentioned methods as below.

3.1 Biorthogonal wavelet full-approximation scheme (BWFAS)

The same procedure is applied as explained in the Briggs et al. [5]. Instead of using Restriction and Prolongation matrices, we use biorthogonal wavelet intergrid operators as, Biorthogonal wavelet restriction operator:

$$Bwr = \begin{bmatrix} h_0 & h_1 & h_2 & h_3 & 0 & 0 & . & . & . & 0 & h_{-1} \\ g_0 & g_1 & 0 & 0 & . & . & . & . & . & 0 & g_{-1} \\ 0 & h_{-1} & h_0 & h_1 & h_2 & h_3 & 0 & . & . & . & 0 \\ 0 & g_{-1} & g_0 & g_1 & 0 & 0 & . & . & . & . & 0 \\ . & & & . & & & . & & & . & \\ . & & & . & & & . & & & . & \\ . & & & . & & & . & & & . & \\ 0 & . & . & . & h_{-1} & h_0 & h_1 & h_2 & h_3 & 0 & 0 \\ 0 & . & . & . & g_{-1} & g_0 & g_1 & 0 & . & . & 0 \end{bmatrix}_{\frac{N}{2} \times N},$$

and Biorthogonal wavelet prolongation operator:

$$Bwp = \begin{bmatrix} \tilde{h}_0 & \tilde{h}_1 & 0 & 0 & . & . & . & & & 0 & \tilde{h}_{-1} \\ \tilde{g}_0 & \tilde{g}_1 & \tilde{g}_2 & \tilde{g}_3 & 0 & . & . & . & & 0 & \tilde{g}_{-1} \\ 0 & \tilde{h}_{-1} & \tilde{h}_0 & \tilde{h}_1 & 0 & . & . & . & & 0 & 0 \\ 0 & \tilde{g}_{-1} & \tilde{g}_0 & \tilde{g}_1 & \tilde{g}_2 & \tilde{g}_3 & 0 & . & . & . & 0 \\ . & & & . & & & . & & & . & \\ . & & & . & & & . & & & . & \\ . & & & . & & & . & & & . & \\ 0 & . & . & . & 0 & \tilde{h}_{-1} & \tilde{h}_0 & \tilde{h}_1 & 0 & 0 & 0 \\ 0 & . & . & . & 0 & \tilde{g}_{-1} & \tilde{g}_0 & \tilde{g}_1 & \tilde{g}_2 & \tilde{g}_3 & 0 \end{bmatrix}^{T}_{\frac{N}{2} \times N}.$$

Step 1: From the system Eq. (1), we get the approximate solution $\tilde{P}_{ij}$ for P_{ij} . Now we find the residual as

$$r_{N \times N} = f_{N \times N} - A(\tilde{P}_{ij})_{N \times N}. \tag{2}$$

Step 2:

$$r_{\frac{N}{2}\times\frac{N}{2}} = Restr_{\frac{N}{2}\times N} r_{NXN} Prolg_{N\times\frac{N}{2}}.$$

Similarly,

$$\tilde{P}_{\frac{N}{2}X\frac{N}{2}} = Restr_{\frac{N}{2}XN} \tilde{P}_{NXN} Prolg_{NX\frac{N}{2}},$$

and

$$A(\tilde{P}_{\frac{N}{2}\times\frac{N}{2}} + e_{\frac{N}{2}\times\frac{N}{2}}) - A(\tilde{P}_{\frac{N}{2}\times\frac{N}{2}}) = r_{\frac{N}{2}\times\frac{N}{2}}. \tag{3}$$

Solve Eq. (3) with initial guess '0', we get $e_{\frac{N}{2}\times\frac{N}{2}}$.

Step 3:

$$r_{\frac{N}{4}\times\frac{N}{4}} = Restr_{\frac{N}{4}\times\frac{N}{2}} r_{\frac{N}{2}\times\frac{N}{2}} Prolg_{\frac{N}{2}\times\frac{N}{4}}.$$

Similarly,

$$\tilde{P}_{\frac{N}{4}\times\frac{N}{4}} = Restr_{\frac{N}{4}\times\frac{N}{2}} \tilde{P}_{\frac{N}{2}\times\frac{N}{2}} Prolg_{\frac{N}{2}\times\frac{N}{4}},$$

and

$$A(\tilde{P}_{\frac{N}{4}\times\frac{N}{4}} + e_{\frac{N}{4}\times\frac{N}{4}}) - A(\tilde{P}_{\frac{N}{4}\times\frac{N}{4}}) = r_{\frac{N}{4}\times\frac{N}{4}}. \tag{4}$$

Solve Eq. (4) with initial guess '0', we get $e_{\frac{N}{4}\times\frac{N}{4}}$.

Step 4: The following procedure is continue up to the coarsest level. We have

$$r_{1X1} = Restr_{1\times 2} r_{2\times 2} Prolg_{2\times 1}.$$

Similarly,

$$\tilde{P}_{1\times 1} = Restr_{1\times 2} \tilde{P}_{2\times 2} Prolg_{2\times 1},$$

and

$$A(\tilde{P}_{1\times 1} + e_{1\times 1}) - A(\tilde{P}_{1\times 1}) = r_{1\times 1}. \tag{5}$$

Solve Eq. (5) we get, $e_{1\times 1}$.

Step 5: Interpolate error up to the finer level, i.e.,

$$e_{2\times 2} = Prolg_{2\times 1} e_{1\times 1} Restr_{1\times 2},$$

$$e_{4\times 4} = Prolg_{4\times 2} e_{2\times 2} Restr_{2\times 4},$$

and so on, we have

$$e_{N\times N} = Prolg_{N\times\frac{N}{2}} e_{\frac{N}{2}\times\frac{N}{2}} Restr_{\frac{N}{2}\times N}.$$

Step 6: Correct the solution using error, $P_{N\times N} = \tilde{P}_{N\times N} + e_{N\times N}$. This is the required solution of the given partial differential equation.

3.2 New biorthogonal wavelet full-approximation scheme (NBWFAS)

Here also the same procedure is applied as explained in the above methods. Instead of using $'Restr'$ and $'Prolg'$ matrices, we use new biorthogonal wavelet intergrid operators as,
New biorthogonal wavelet restriction operator:

$$NBwr = \begin{bmatrix} h_0 & 0 & h_1 & 0 & h_2 & 0 & h_3 & 0 & . & . & . & 0 & h_{-1} & 0 \\ 0 & 1 & 0 & 0 & . & . & . & & & . & . & . & & 0 \\ g_0 & 0 & g_1 & 0 & 0 & . & . & . & 0 & 0 & 0 & g_{-1} & & 0 \\ 0 & 0 & 0 & 1 & 0 & . & . & . & & . & . & . & & 0 \\ . & & & & . & & & & . & & & . & & \\ . & & & & . & & & & . & & & . & & \\ . & & & & . & & & & . & & & . & & \\ 0 & . & 0 & h_{-1} & 0 & h_0 & 0 & h_1 & h_2 & 0 & h_3 & 0 & . & 0 \\ 0 & 0 & . & . & . & 0 & 1 & 0 & . & . & . & & 0 & 0 \\ 0 & . & 0 & g_{-1} & 0 & g_0 & 0 & g_1 & 0 & . & . & . & 0 & 0 \\ 0 & 0 & & . & . & . & & 0 & 1 & 0 & . & . & . & 0 \end{bmatrix}_{\frac{N}{2}\times N},$$

and New reconstruction matrix:

$$NBwp = \begin{bmatrix} \tilde{h}_0 & 0 & \tilde{h}_1 & 0 & & & . & . & . & & 0 & \tilde{h}_{-1} & 0 \\ 0 & 1 & 0 & 0 & . & . & . & & & . & . & . & 0 \\ \tilde{g}_0 & 0 & \tilde{g}_1 & 0 & \tilde{g}_2 & 0 & \tilde{g}_3 & 0 & . & . & . & 0 & \tilde{g}_{-1} & 0 \\ 0 & 0 & 0 & 1 & 0 & . & . & . & & . & . & . & 0 \\ . & & & & . & & & . & & & . & & \\ . & & & & . & & & . & & & . & & \\ . & & & & . & & & . & & & . & & \\ 0 & . & 0 & \tilde{h}_{-1} & 0 & \tilde{h}_0 & 0 & \tilde{h}_1 & 0 & . & . & . & 0 & 0 \\ 0 & 0 & . & . & . & 0 & 1 & 0 & . & . & . & & 0 & 0 \\ 0 & . & 0 & \tilde{g}_{-1} & 0 & \tilde{g}_0 & 0 & \tilde{g}_1 & 0 & \tilde{g}_2 & \tilde{g}_3 & 0 & . & 0 \\ 0 & 0 & & . & . & . & & 0 & 1 & 0 & . & . & . & 0 \end{bmatrix}_{\frac{N}{2}\times N}.$$

4 Numerical experiments

Here, we present two test EHL problems, which show the efficiency of WFAS.
Test Problem 1. Consider the elasto-hydrodynamic lubrication with line contact problem [1],

$$\frac{\partial}{\partial x}(\varepsilon(P)\frac{\partial P}{\partial x}) - \frac{\partial}{\partial x}(\rho(P)H(P)) = 0, \tag{6}$$

where $\varepsilon(P) = \frac{\rho(P)H(P)^3}{\lambda\eta(P)}$, $P(x)$ and $H(x)$ are unknown pressure and film thickness, λ a dimensionless speed parameter, $\lambda = \frac{12p_0VR^2}{b^2p_h}$. The boundary conditions are given as follows.

$$P(x_a) = P(x_b) = \frac{\partial P(x_c)}{\partial x} = 0. \tag{7}$$

The domain of the problem is from the inlet x_a to the cavitation point x_b. Boundary conditions of zero pressure are imposed at x_a and x_b. The nondimensional film thickness equation is given, in integral form as

$$H(x) = H_{00} + \frac{x^2}{2} - \frac{1}{\pi}\int_{x_a}^{x_b} \log|x - x'|P(x')dx', \tag{8}$$

where H_{00} is the central offset film thickness, the second term defines the undeformed contact shape and the integral term represents the elastic deformation of the contact.

The nondimensional force balance equation, given by

$$\int_{x_a}^{x_b} P(x)dx = \frac{\pi}{2}, \tag{9}$$

represents the balance between the applied load and the total internal pressure in the lubricant. The nondimensional form for viscosity $\eta(P)$, which was established by Roelands [16], and density $\rho(P)$, which was presented by Dowson and Higginson [11], are

$$\rho(P) = \frac{0.59e+9+1.34Pp_h}{0.59e+9+Pp_h},\ \eta(P) = exp(\frac{\alpha p_0}{z}[-1+(1+\frac{Pp_h}{p_0})^z]), \tag{10}$$

where $z = 0.6$ is the viscosity index, $\alpha = 2.165e-8$ is the pressure viscosity index, $p_0 = 1.98e+8$ is the ambient pressure and $p_h = 1.84e+9$ is the maximum Hertzian pressure. The three non-dimensional physical parameters that characterize the line contact problem are velocity (U), load force (W) and elasticity (G). The equations (6)-(9) are discretized using finite differences with uniform grid of N points $x_i, 1 \le i \le N$, and the domain of interest is $[x_a, x_b] = [-5, 2.5], x_c$ is the cavitation point, to be determined in the solution process, is an internal point near exit. The discretized form of Reynolds equation is as

$$\frac{(\frac{\varepsilon_i+\varepsilon_{i+1}}{2})(\frac{P_{i+1}-P_i}{\Delta x}) - (\frac{\varepsilon_i+\varepsilon_{i-1}}{2})(\frac{P_i-P_{i-1}}{\Delta x})}{\Delta\ x} - \frac{\rho_i H_i - \rho_{i-1}H_{i-1}}{\Delta\ x} = 0, \tag{11}$$

where $\varepsilon_i = \frac{\rho_i H_i^3}{\lambda \eta_i}$. The film thickness equation approximated at x_i on the regular grid is given by

$$H(x_i) = H_{00} + \frac{x_i^2}{2} - \frac{1}{\pi}\sum_{j=1}^{N} K_{ij} P(x_j), \tag{12}$$

where

$$\begin{aligned} K_{ij} &= (x_i - x_j + \frac{\triangle x}{2})(log|x_i - x_j + \frac{\triangle x}{2}| - 1) \\ &\quad -(x_i - x_j - \frac{\triangle x}{2})(log|x_i - x_j - \frac{\triangle x}{2}| - 1), \end{aligned} \tag{13}$$

for $i = 0, 1, \ldots, N$ and $j = 0, 1, \ldots, N$ and the force balance equation in discrete from is

$$\triangle x \sum_{j=0}^{N-1} (\frac{P_j + P_{j+1}}{2}) - \frac{\pi}{2} = 0. \tag{14}$$

Discretizing Eqs. (6) and (8) a piecewise constant form of $P(x)$ is assumed. The boundary conditions are

$$P(x_a) = 0, \quad \frac{dP}{dx}|_{x=x_c} \geq 0. \tag{15}$$

Using these boundary conditions we take Eqns. (11), (12) and (14) together in the form of $A(P_{ij}) = f_{ij}$. To solve this equation as explained in Section 3, we get the numerical solutions presented in Figure 1. Comparison of residual v/s iterations is given in Figure 2 and residual with iterations for different N are presented in Table 1. And also, comparison of CPU time for different schemes is given in Table 3.

Test Problem 2. We consider the dimensionless Reynolds equation of elasto-hydrodynamic lubrication point contact problem [21],

$$\frac{\partial}{\partial x}(\varepsilon \frac{\partial P}{\partial x}) + \alpha^2 \frac{\partial}{\partial y}(\varepsilon \frac{\partial P}{\partial y}) - \frac{\partial}{\partial x}(\rho' H) = 0, \tag{16}$$

where $\varepsilon = \frac{\rho' H^3}{\lambda \eta'}$, $P(x, y)$ and $H(x, y)$ are unknown pressure and film thickness, x is the dimensionless coordinate ($x = \frac{X}{a}$, a is the half length of the elliptic contact area in the x direction), y is the dimensionless coordinate ($y = \frac{Y}{b}$, b is the half length of the elliptic contact area in the y direction), λ is the dimensionless speed parameter, $\lambda = \frac{12\eta_0 U R_x^2}{a^3 p_h K_{ex}^2}$. η' is dimensionless

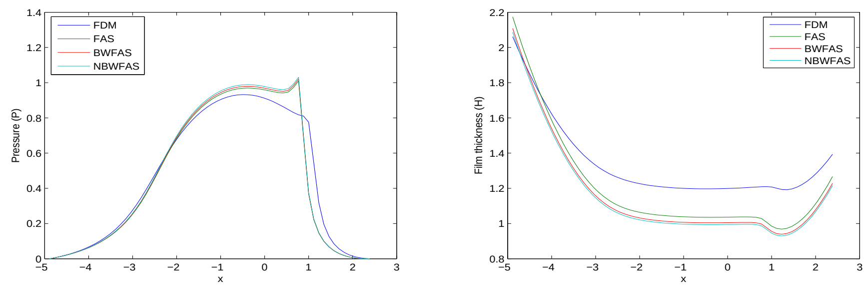

Figure 1: Comparison of numerical solutions for $N = 256$ of Test Problem 1.

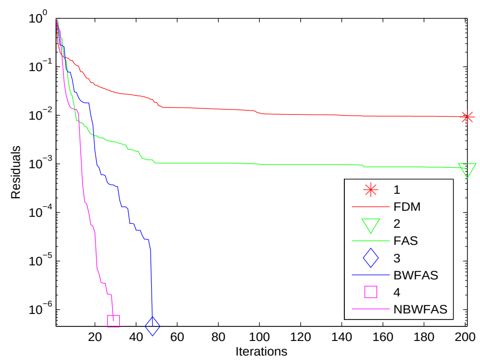

Figure 2: Comparison of residual v/s iterations for $N = 128$ of Test Problem 1.

lubricant viscosity ($\eta' = \frac{\eta}{\eta_0}$), ρ' is dimensionless lubricant density ($\rho' = \frac{\rho}{\rho_0}$), K_{ex} is the elliptic coefficient of the surface in the x direction, α is a ratio parameter ($\alpha = \frac{a}{b}$), P is dimensionless pressure ($P = \frac{p}{p_h}$), p_h is the maximum Hertzian contact stress and H is the dimensionless film thickness ($H = \frac{hR_x}{a^2}$). The boundary conditions of (16) are, Inlet boundary conditions $P(x_a, y) = 0$, Outlet boundary conditions $P(x_b, y) = 0$ and $\frac{\partial P(x_b,y)}{\partial x} = 0$, Side boundary conditions $P(x, y_a) = P(x, -y_b) = 0$, where x_a and x_b are the dimensionless coordinates of the inlet and outlet, x_a is given but x_b should be determined by the outlet boundary conditions and $y = \pm 1$ are the two sides of the contact region. The Film thickness equation is given, in integral form as

$$H(x, y) = H_{00} + \frac{x^2 + y^2}{2} - \frac{2}{\pi^2} \int_{x_a}^{x_b} \int_{y_a}^{y_b} \frac{P(S, T)dSdT}{\sqrt{(x - S)^2 + (y - T)^2}}, \qquad (17)$$

where H_{00} is the central offset film thickness, the second term defines the undeformed contact shape and the integral term represents the elastic deformation of the contact.

The dimensionless Force balance equation, given by

$$\int_{x_a}^{x_b}\int_{y_a}^{y_b} P(x,y)dxdy = \frac{2\pi}{3}, \tag{18}$$

which represents the balance between the applied load and the total internal pressure in the lubricant. The dimensionless form for viscosity η' , which was established by Roelands [16], and density ρ' , which was presented by Dowson and Higginson [11], are

$$\rho' = (1+\frac{0.6P}{1+1.7P}), \quad \eta' = \exp\left(\ln(\eta_0)+9.67\right)[-1+(1+5.1e-9Pp_h)^z],$$

where $z = 0.68$ is the viscosity index, $\eta_0 = 1.98e{+}08$ is the ambient pressure and $p_h = 1.84e+09$ is the maximum Hertzian pressure, α is the ratio of a and b. K_{ex} is the relative curvature in the x direction. For the equivalent curvature of the point contact, $K_{ex} = 1$. The following discussions are based on $\alpha = 1$. The finite difference discretization of Eq. (16) can be written as

$$\begin{aligned}
&\left\{\frac{(\frac{\varepsilon_{i,j}+\varepsilon_{i-1,j}}{2})P_{i-1,j}+(\frac{\varepsilon_{i,j}+\varepsilon_{i+1,j}}{2})P_{i+1,j}-(2\varepsilon_{i,j}+\varepsilon_{i-1,j}+\varepsilon_{i+1,j})P_{ij}}{\triangle\, x^2}\right\}\\
&+\alpha^2\left\{\frac{(\frac{\varepsilon_{i,j}+\varepsilon_{i,j-1}}{2})P_{i,j-1}+(\frac{\varepsilon_{i,j}+\varepsilon_{i,j+1}}{2})P_{i,j+1}-(2\varepsilon_{i,j}+\varepsilon_{i,j-1}+\varepsilon_{i,j+1})P_{ij}}{\triangle\, y^2}\right\}\\
&\qquad-\left\{\frac{\rho'_{i,j}H_{i,j}-\rho'_{i-1,j}H_{i-1}}{\triangle\, x}\right\}=0.
\end{aligned} \tag{19}$$

The film thickness equation becomes

$$H_{ij} = H_{00} + \frac{x_i^2+y^j}{2} + \frac{2}{\pi^2}\sum_{k=1}^{N}\sum_{l=1}^{N} D_{ij}^{kl}P_{kl}, \tag{20}$$

where D_{ij}^{kl} is the stiffness coefficient of the elastic deformation

$$\begin{aligned}
D_{ij}^{kl} &= (x_i - x_j + \frac{\triangle\, x}{2})(log|x_i - x_j + \frac{\triangle\, x}{2}| - 1)\\
&\quad -(x_i - x_j - \frac{\triangle\, x}{2})(log|x_i - x_j - \frac{\triangle\, x}{2}| - 1)\\
&\quad (y_k - y_l + \frac{\triangle\, y}{2})(log|y_k - y_l + \frac{\triangle\, y}{2}| - 1)\\
&\quad -(y_k - y_l - \frac{\triangle\, y}{2})(log|y_k - y_l - \frac{\triangle\, y}{2}| - 1),
\end{aligned} \tag{21}$$

for $i, k = 0, 1, \ldots, N$ and $j, l = 0, 1, \ldots, N$ the force balance equation which as

$$\triangle x \triangle y \sum_{i=1}^{N}\sum_{j=1}^{N} P_{ij} = \frac{2\pi}{3}, \tag{22}$$

three non-dimensional physical parameters that characterize the point contact problem are velocity (U), load force (W) and elasticity (G). To solve equations (19), (20) and (22) as explained in Section 3, we get the numerical solutions presented in Figure 3 and Figure 4, pressure and film thickness, respectively. Comparison of residual with iterations for different N is presented in Table 2. And also, comparison of CPU time for different schemes is given in Table 3.

Table 1: Comparison of residual with iterations of different schemes of the Test Problem 1.

		Residual (Iterations)		
N	FDM	FAS	BWFAS	NBWFAS
16	2.11e-01(21)	3.78e-03(10)	5.34e-05(6)	3.98e-05(5)
32	9.91e-01(39)	8.13e-03(30)	5.42e-06(15)	4.01e-06(10)
64	1.83e-02(75)	2.42e-04(59)	9.28e-06(34)	7.15e-07(22)
128	9.26e-02(200)	8.08e-04(135)	4.57e-07(48)	5.79e-07(29)
256	1.40e-03(289)	9.11e-05(198)	5.71e-08(63)	7.42e-08(31)

Table 2: Comparison of residual with iterations of different schemes of the Test Problem 2.

		Residual (Iterations)		
N	FDM	FAS	BWFAS	NBWFAS
8	7.32e-03(173)	5.92e-04(65)	2.72e-04(47)	9.98e-05(41)
16	2.23e-03(214)	8.85e-05(188)	6.82e-05(91)	4.92e-05(84)
32	7.45e-04(259)	6.89e-05(201)	8.65e-06(112)	5.90e-06(98)
64	6.51e-04(286)	4.84e-05(215)	3.01e-06(154)	1.98e-06(121)
128	4.40e-05(315)	8.13e-06(250)	1.10e-06(159)	8.13e-07(126)

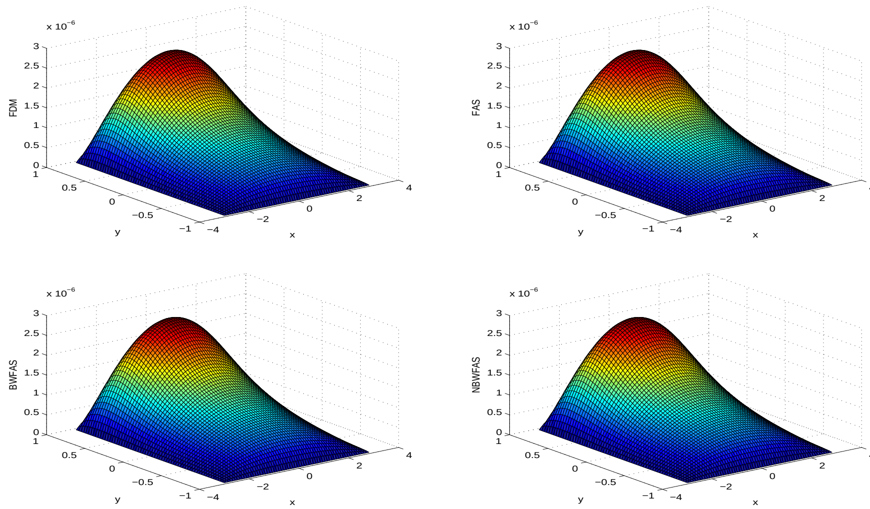

Figure 3: Pressure numerical solutions comparison for $N = 64$ of equation (19).

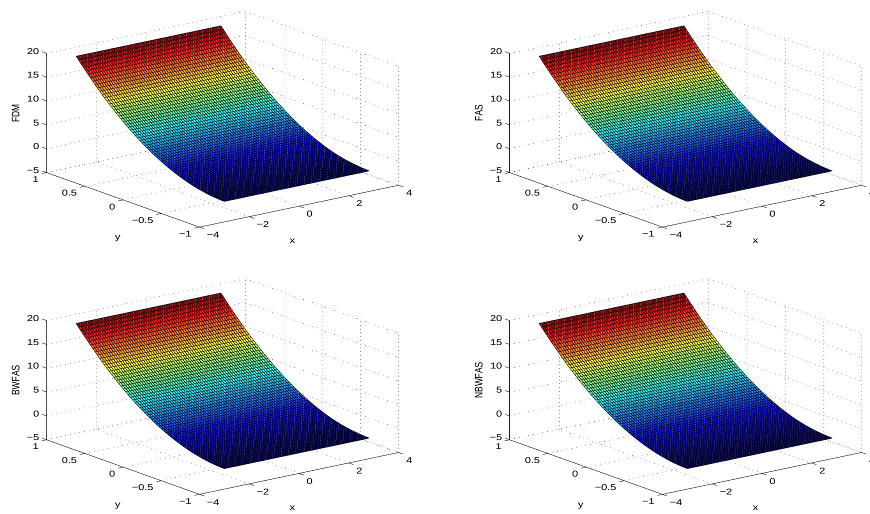

Figure 4: Film thickness numerical solution comparison for $N = 64$ of equation (20).

5 Conclusion

In this paper, we have introduced an efficient biorthogonal wavelet-based full-approximation schemes for the numerical solution of EHL line and point

Table 3: The comparison of CPU time (in seconds) of the different methods.

Problem	Method	Setup time	Running time	Total time
	FDM	9.10	7.21	16.31
Test Problem 1	FAS	8.01	5.53	13.54
(N=256)	BWFAS	7.24	3.98	11.22
	NBWFAS	7.21	2.64	9.85
	FDM	11.28	8.13	19.41
Test Problem 2	FAS	10.89	6.41	17.30
(N=64)	BWFAS	9.01	4.62	13.63
	NBWFAS	8.54	3.05	11.59

contact problems. Solutions obtained from the figures looking like similar but from the tables, we found that residual error of the proposed schemes decreases in less number of iteration then the existing methods. Also from the last table, the presented schemes give better solutions with fast convergence in less computational time compared to standard techniques (FDM and FAS), which have been demonstrated through the tested problems. Hence the biorthogonal wavelet methods are very efficient and convenient for the numerical solution of differential equations arising in fluid dynamics.

Acknowledgements

We are thankful to the anonymous reviewers for their valuable suggestions.

References

[1] S. Ahmed, C.E. Goodyer, P.K. Jimack, *An efficient preconditioned iterative solution of fully-coupled elastohydrodynamic lubrication problems*, Appl. Numer. Math. **62** (2012) 649-663.

[2] A. Avudainayagam, C. Vani, *Wavelet based multigrid methods for linear and nonlinear elliptic partial differential equations*, Appl. Math. Comput. **148** (2004) 307–320.

[3] G. Beylkin, R. Coifman, V. Rokhlin, *Fast wavelet transforms and numerical algorithms-I*, Commun. Pure Appl. Math. **44** (1991) 141-183.

[4] A. Brandt, *Multi-level adaptive solutions to boundary-value problems*, Math. Comp. **31** (1977) 333-390.

[5] W.L. Briggs, V. E. Henson, S. F. McCormick, *A multigrid tutorial (2nd ed.)*, SIAM, Philadelphia, 2000.

[6] N.M. Bujurke, C.S. Salimath, R.B. Kudenatti, S.C. Shiralashetti, *Analysis of modified Reynolds equation using the wavelet-multigrid scheme*, Numer. Methods Partial Differential Equations **23:3** (2006) 692–705.

[7] N.M. Bujurke, C.S. Salimath, R.B. Kudenatti, S.C. Shiralashetti, *Wavelet-multigrid analysis of squeeze film characteristics of poroelastic bearings*, J. Comput. Appl. Math. **203:1** (2007) 237-248.

[8] N.M. Bujurke, C.S. Salimath, R.B. Kudenatti, S.C. Shiralashetti, *A fast wavelet-multigrid method to solve elliptic partial differential equations*, Appl. Math. Comput. **185:1** (2007) 667-680.

[9] S.C. Burrus, A.G. Ramesh, G. Haitao, *Introduction to wavelets and wavelet transform-A primer*, Prentice Hall International, 1998.

[10] A. Choen, I. Daubechies, J. Feauvean, *Biorthogonal based of compactly supported wavelets*, Comm. Pure Appl. Math. **45** (1992) 485-560.

[11] D. Dowson, G.R. Higginson, *Elasto-Hydrodynamic lubrication, The Fundamentals of Roller and Gear Lubrication*, Pergaman Press Oxford, Great Britain, 1966.

[12] W. Hackbusch, U. Trottenberg, *Multigrid Methods*, Springer-Verlag, Berlin, 1982.

[13] A.A. Lubrecht, *Numerical solution of the EHL line and point contact problem using multigrid techniques*, Ph.D. Thesis, University of Twente, Enschede, The Netherlands, 1987.

[14] P.M. Lugt, G.E. Morales-Espejel, *A review of elasto-hydrodynamic lubrication theory*, Trib. Trans. **54** (2011) 470-496.

[15] A.I. Petrusevich, *Fundamental conclusions from the contact hydrodynamic theory of lubrication*, Izv. Akad, Nauk SSR (OTN) **3** (1951) 209-223.

[16] C.J.A. Roelands, *Correlational aspects of the viscosity-temperature-pressure relationship of lubricating oils*, Ph. D. Thesis, Technische Hogeschool Delft, V.R.B., Groningen, The Netherlands, 1996.

[17] D.K. Ruch, P.J.V. Fleet, *Wavelet theory an elementary approach with applications*, John Wiley and Sons, 2009.

[18] W. Sweldens, *The construction and application of wavelets in numerical analysis*, PhD. Thesis, Department of Computer Science, Katholieke Universiteit Leuven, Belgium, 1994.

[19] U. Trottenberg, C. Oosterlee, A. Schuller, *Multigrid*, Academic Press London, San Diego, 2001.

[20] C.H. Venner, A.A. Lubrecht, *Multilevel methods in lubrication*, Elsevier, 2000.

[21] C.H. Venner, *Multilevel solution of the EHL line and point contact problems*, PhD. Thesis, University of Twente, The Netherlands, 1991.

[22] P. Wesseling, *An introduction to multigrid methods*, John Wiley, Chichester, 1992.

[23] E.A. Zargari, P.K. Jimack, M.A. Walkley, *An investigation of the film thickness calculation for elastohydrodynamic lubrication problems*, Arthur et al. (editors) Proceedings of the 9th Conference on Numerical Methods for Fluid Dynamics; ICFD 2007.